Original article

Protective effect of eriodictyol against hyperglycemia-induced diabetic nephropathy in rats entails antioxidant and anti-inflammatory effects mediated by activating Nrf2

Jozaa Z. AlTamimi [a], Nora A. AlFaris [a,*], Ghedeir M. Alshammari [b], Reham I. Alagal [c], Dalal H. Aljabryn [a], Mohammed Abdo Yahya [b]

[a] Department of Physical Sports Sciences, College of Education, Princess Nourah Bint Abdulrahman University, P.O. Box 84428, Riyadh 11671, Saudi Arabia
[b] Department of Food Science and Nutrition, College of Food and Agricultural Sciences, King Saud University, P.O. Box 84428, Riyadh 11451, Saudi Arabia
[c] Department of Health Sciences, College of Health and Rehabilitation Sciences, Princess Nourah Bint Abdulrahman University, P.O. Box 84428, Riyadh 11671, Saudi Arabia

ABSTRACT

The pathogenesis of diabetic nephropathy (DN) involves cellular activation of oxidative stress and inflammation. Eriodictyol is a citrus-derived flavonoid with multiple pharmacological and protective effects in various conditions. The protective role of Eriodictyol against diabetes and diabetic nephropathy is less investigated. The current research aimed to explore the role of eriodictyol in protecting against DN prompted by streptozotocin in male rats and investigate some possible mechanisms of action. Diabetes was brought about in rats by an i.p injection of a lone dose (65 mg/kg). Five groups of rats were included (n = 8 each) as control (non-diabetic), eriodictyol (20 mg/kg, orally), STZ-diabetic, STZ + eriodictyol (20 mg/kg, orally), and STZ + eriodictyol (20 mg/kg, orally) + ML385 (30 μg/kg, i.p.). Kidney histology and the levels of some markers of kidney function, renal oxidative stress, and renal inflammation were analyzed in all groups of rats. Treatment with eriodictyol prevented the damage in the renal glomeruli and tubules and reduced renal immune cell infiltration in STZ-treated animals. It also spiked urinary creatinine excretion and reduced urine volume and urinary levels of albumin, monocyte chemoattractant protein 1 (MCP-1), urinary kidney injury molecule-1 (KIM-1), and nephrin in these diabetic rats. In addition, eriodictyol stimulated the nuclear protein accumulation of Nrf2 and boosted the expression of superoxide dismutase (SOD), glutathione (GSH), heme oxygenase-1 (HO-1), and catalase (CAT) in the diabetic rat kidneys. In concomitance, it reduced the nuclear levels of NF-κB and levels of interleukine-6 (IL-6), malondialdehyde (MDA), and tumor necrosis factor-α (TNF-α) and attenuated the reduction in renal ATP levels and the increase in the mitochondria transition pore opening (mtTPT). However, the administration of eriodictyol did not affect rats' body weights and fasting glucose and insulin levels but significantly reduced serum levels of cholesterol, triglycerides, LDL-c, and oxidized LDL-c (ox-LDL-c). In conclusion, eriodictyol prevents STZ-induced nephropathy by a hypolipidemic effect and concomitant antioxidant and anti-inflammatory effects mediated by activating Nrf2/NF-κB/antioxidant axis.

* Corresponding author.
E-mail addresses: jzaltamimi@pnu.edu.sa (J.Z. AlTamimi), naalfaris@pnu.edu.sa (N.A. AlFaris), aghedeir@ksu.edu.sa (G.M. Alshammari), rialagal@pnu.edu.sa (R.I. Alagal), dhaljabryn@pnu.edu.sa (D.H. Aljabryn), mabdo@ksu.edu.sa (M. Abdo Yahya).
Peer review under responsibility of King Saud University.

1. Introduction

Type 1 diabetes (T1DM) is a metabolic disorder that affects carbohydrate and lipid metabolism and is induced by the immune system-mediated damage to β-cells in the pancreas (Giwa et al., 2020). During the progression of T1DM, there is a sustained state of hyperglycemia, hyperlipidemia, and inflammation, which all together induce multi-organ damage and microvascular and microvascular complications (Giwa et al., 2020). End-stage renal disease (ESRD) is primarily brought on by diabetic nephropathy (DN), which is the foremost and most frequent consequence of

type 1 diabetes (T1DM) (Zoja et al., 2020). Major clinical findings in patients with DN include progressive glomerular hyperfiltration and hypertrophy, mesangial cell expansion, a drop in the glomerular filtration rate (GFR), tubular damage, interstitial fibrosis, and albuminuria (Zoja et al., 2020).

Hyperglycemia-mediated profuse production of reactive oxygen species (ROS), leading to consequent oxidative stress, is the driving force underlying the multi-organ and renal damage in patients with T1DM (Rico-Fontalvo et al., 2022). The adverse effects of ROS not only promote DNA and membrane damage but induce hyperlipidemia and cellular inflammation, necrosis, and apoptosis (Tuttle et al., 2022). In this regard, it has been demonstrated that hyperglycemia induces massive amounts of ROS in the majority of tissues by activating several mechanisms. These mechanisms include impairing mitochondrial oxidative phosphorylation, increasing the generation of advanced glycation products (AGEs), and stimulating diverse ROS-generating pathways like polyol, hexose monophosphate, and protein kinase C (PKC) pathways (Jha et al., 2016; Tuttle and Alicic, 2021). However, attenuating oxidative stress with natural antioxidants alleviated the majority of diabetic complications and mitigated damage to renal glomeruli and tubules and all other renal dysfunctions in experimental animals of T1DM (Tavafi, 2013; Bolignano et al., 2017; Mahmoodnia et al., 2017; Al-Waili et al., 2017; Kandhare et al., 2017).

In addition, hyperglycemia-induced DN and multi-organ damage are associated with the attenuation of the cellular antioxidant mechanisms and the scavenging of antioxidants in the cells, both enzymatically and non-enzymatically. Indeed, accumulating lines of evidence have shown that DN is caused by an imbalance in ROS generation versus scavenging antioxidants in cells (Miranda-Díaz et al., 2016; Kandhare et al., 2017; Shukla et al., 2018; Hernandez et al., 2022). In addition, DN is characterized by altered antioxidant signaling pathways. In the kidneys, as well as in the majority of other systemic cells, the nuclear factor erythroid-derived 2-like 2 (NRF2) is the main antioxidant transcription factor that fights oxidative stress by promoting the glutathione (GSH) expression and certain types of antioxidant enzymes, including glutathione peroxidase (GPX), superoxide dismutase (SOD), heme oxygenase-1 (HO-1), and catalase (CAT) (Baird and Yamamoto, 2020). Under the basal condition, Nrf2 activity is controlled by binding to the Kelch-like ECH-associated protein 1 (Keap-1), which is a natural inhibitor that sequesters and promotes the ubiquitination and cytoplasmic degradation of Nrf2 (Ulasov et al., 2022). Yet, in response to oxidative stress, Nrf2 is released from keap-1 and translocates to the nucleus to initiate the antioxidant transcription process (Ulasov et al., 2022). However, Nrf2/antioxidant signaling is unexpectedly impaired in diabetic rats' kidneys after chronic exposure to hyperglycemia (Chen et al., 2019; Mohan et al., 2020; Li et al., 2021; Xing et al., 2021). In addition, the deletion of Nrf2 intensified oxidative and inflammatory damage and increased the degree of cell apoptosis, fibrosis, and albuminuria in the kidneys of streptozotocin-enhanced T1DM rats (Jiang et al., 2010; Zheng et al., 2011). In contrast, independent of modulating blood glucose levels, the activation of Nrf2 alone attenuated the histological alteration and function impairments in the kidneys and slowed down the advancement of the DN in diabetic animals by muzzling inflammation, oxidative stress, and hyperlipidemia (Sun et al., 2017; Dong et al., 2017; Chen et al., 2019; Li et al., 2021; Xing et al., 2021). Therefore, searching for drugs that can induce Nrf2 activation seems to be an ideal drug to alleviate or suppress the progression of DN.

Currently, no definite therapy to treat DN exists, even with controlling hyperglycemia. The treatment with angiotensin II receptor blocker (e.g., valsartan), an angiotensin receptor–neprilysin inhibitor (LCZ696), and statins showed very effective protection in diabetic animal models by attenuating the renal oxidative stress, inflammation, and apoptosis (Mohany et al., 2020; Mohany et al., 2022a; Huang et al. 2023). Recently, much attention has been given to the role of plants' flavonoids in treating chronic kidney dysfunctions and DN due to their antioxidant potential (Hu et al., 2021; Lin et al., 2022). Further, several plant flavonoids alleviated DN by activating the Nrf2/antioxidant axis and suppressing the NF-κB signaling pathway (Chen et al., 2019; Ding et al., 2020). Examples include berberine, ursolic acid, naringenin, apigenin, genistein, rutin, proanthocyanin, betulinic acid, and statins (Mohany et al., 2022b).

Eriodictyol is the major flavanone isolated from citrus fruits (Buranasudja et al., 2022). Eriodictyol has been found to have several pharmacological activities, including hypoglycemic, hypolipidemic, antioxidant, and anti-inflammatory protective impacts of eriodictyol have been reported in the animals' brains, livers, lungs, kidneys, and hearts (Deng et al., 2020; Islam, 2020). However, the protective influence of eriodictyol against diabetic health problems was less investigated and few studies exist. In this regard, the hypoglycemic impact of eriodictyol was probably due to its capability to spur peripheral insulin sensitivity and glucose uptake (Kwon and Choi, 2019). In addition, eriodictyol also prevented early retinal damage in STZ-treated rats via an antioxidant potential (Bucolo et al., 2012). Nonetheless, the capability of eriodictyol to prompt Nrf2 signaling was explored in multiple animal studies, and the major mechanism underlying its protective potential was shown (Johnson et al., 2009; Jing et al., 2013; Li et al., 2016; Lv et al., 2019; Li et al., 2022).

Despite the information above, the protective effect of eriodictyol against DN has never tested before. Interestingly, in a single in vitro study, eriodictyol inhibited HG-induced glomerular mesangial cell death and fibrosis by reducing ROS, attenuating oxidative stress, and blocking the production of inflammatory cytokines (Bai et al., 2019). Accordingly, this research was conducted to explore whether eriodictyol can also attenuate renal function and structure impairment in STZ diabetic rats. We also investigated the precise mechanism of action by focusing on its hypoglycemic impact as well as its potential to activate the Nrf2 antioxidant axis.

2. Materials and methods

2.1. Animals

Forty adult male Wistar rats, ages 10 weeks and weighing 180–200 g, were employed to conduct the animal experiment. All animals were provided by the Experimental Animal Care Center at King Saud University, Riyadh, Saudi Arabia, and were kept there throughout. The trial rats were placed in a spate room with automatic controls for the room's temperature, humidity, and day/light cycle of 22 ± 1 °C, 55–60%, and 12 h/12 h, respectively. All protocols regarding animal treatment, surgery, and blood/tissue collections were authorized by the official review board at Princess Nourah University, Riyadh, KSA (IRB Number 20–0096), which conformed to the standards specified by the US National Institutes of Health.

2.2. Establishment of the diabetic animal model

To induce an insulin deficiency in rats, we followed the protocols of others using a single dose of STZ. Accordingly, STZ powder (Cat. No. S0130) from Sigma Aldrich, St Louis, MO, USA, was obtained and freshly dissolved in a slightly acidic Na-citrate buffer solution (pH = 5.5). Rats were injected with a single intraperitoneal dose of STZ-solution at a final concentration of 65 mg/kg. In addition, rats were given a 0.5% glucose solution to inhibit death from acute hypoglycemia. Three days following the STZ injection, fasting

blood glucose (FBG) levels were measured using a glucometer. Rats who had FBG levels of>300 mg/kg were considered diabetic and were selected for further animal trials.

2.3. Experimental design

Eriodictyol (Cat. 94258) from Sigma Aldrich, USA) was obtained and dissolved in 0.5% carboxymethyl cellulose. Non-diabetic and STZ-diabetic rats were selected and divided randomly into five groups (8 rats each). These groups were: (1) the control non-diabetic group: rats were only administered 0.5% carboxymethyl cellulose to serve as a vehicle; (2) the eriodictyol-treated non-diabetic group: non-diabetic control rats were treated with eriodictyol at a final dose (20 mg/kg). (3) STZ-diabetic group: rats with DM were administered carboxymethyl cellulose only; (4) STZ + e riodictyol-treated group: diabetic rats that were treated with eriodictyol (20 mg/kg); (5) STZ + eriodictyol + ML385-treated group: rats with DM were treated intraperitoneally with ML385 (30 μg/kg), a selective Nrf2 inhibitor, 1 h before the administration of eriodictyol (20 mg/kg). All treatments were given daily for a total period of 12 weeks.

The eriodictyol or the vehicle was administered to rats orally by gavage. Eriodictyol dosage was determined by reference to prior research that demonstrated Nrf2 activation offered protection against cisplatin-induced nephropathy (Li et al., 2016). ML385 at the selected dose was also used to suppress Nrf2 in vivo in rats Deng et al. (2020). It was also validated to inhibit renal activation of Nrf2 in these rats in our preliminary studies.

2.4. Urine sampling and biochemical analysis

Urine sampling was performed for 24 h on the final day of the experiment after all rats were segregated into metabolic cages (1 rat/cage). After centrifuging the collected urine at 1200 xg for 10 min, the supernatants were separated and kept at 20 °C pending analysis. At this time, urinary albumin levels were measured by a rat-specific ELISA kit (cat 108789, Abcam, Cambridge, UK). Creatinine (Cr) levels in the urine samples were quantified using a rat's specific enzymatic kit (cat 80340, Chrystal Chem, IL, USA). Monocyte chemoattractant protein 1 (MCP-1), urinary kidney injury molecule-1 (KIM-1), and nephrin levels in the were measured (cat ELR-MCP1, RayBiotech, IL, USA, cat 80684, Crystal; Chem USA, and cat CSB-E13957r, CUSABIO, TX, USA).

2.5. Collection of serum and biochemical analysis

All rats underwent anaesthesia using a ketamine/xylazine mixture (80/10 $^v/^v$/kg) after being fasted for 12 h. All rats had their hearts punctured, and blood was collected into plain or EDTA-collection tubes. The collected blood samples were centrifuged (1200 $\times$ g; 10 min) to separate serum and plasma. Serum samples were kept at $-$ 80 °C and used later for various biochemical measurements. Fasting plasma glucose amounts were measured using an assay kit (cat 81693, Chrystal Chem, IL, USA). Fasting plasma insulin levels were measured using an ELISA kit (cat P01323, Ray-Biotech, GA, USA). The same set of kits (cat. 80340, Chrystal Chem, IL, USA, and cat 108789, Abcam, Cambridge, UK) that were used to assess the concentration of Cr and albumin in the urine were also used to measure their levels in the serum. Using a colorimetric kit (Cat. DIUR-100, Bioassay Systems), the levels of serum urea were determined. The following assay kits were used to measure the serum levels of total cholesterol (CHOL) and total triglycerides (TGs), low-density lipoprotein-cholesterol (LDL-c), and high-density lipoprotein-cholesterol (HDL-c), in that order: Cat. 10009582 (Cayman Chemicals, CA, USA), cat. ECCH-100 (BioAssay Systems, CA), cat. 79960 (Crystal Chemicals, TX, USA), and Cat.

79970 (Crystal Chemicals, TX, USA, respectively). All urinary kits used were rat's specific, and all measurements were performed for all experimental groups (8 rats/group).

2.6. Tissue collection and preparation

After blood collection, the rats were ethically killed by cervical dislocation. After opening their abdomens, the kidneys were taken out, placed on ice, and weighed. The kidneys were divided into smaller segments, swiftly frozen in liquid nitrogen, and kept at -80 °C for further processing. Some freshly-collected kidney sections were placed in 10% buffered formalin, transferred to the pathology laboratory at the College of Science at King Saud University, and processed according to standard histology procedures. Later, the nuclear and cytoplasmic fractions of the kidneys were obtained using the cytoplasmic/nuclear extraction kit (Cat. No. 4110147; Bio-Rad, CA, USA). The RNA extraction kit (Cat. # 74004; Qiagen, Germany) was also used to obtain total RNA from the frozen livers.

2.7. Preparation of tissue homogenates

Tissue homogenates for the biochemical analysis were prepared by homogenization of 50 mg of the frozen kidney tissue of each sample in 10 volumes in ice-cold phosphate buffer (pH = 7.4) using a sonicator. The homogenates were centrifuged (12,000 $\times$ g; 15 min; 4 °C) and the supernatants were transferred to new tubes and stored at -80 ℃ until use.

2.8. Biochemical analysis of inflammatory and antioxidant markers in the renal homogenates

Expression levels of tumor necrosis factor-alpha (TNF-α) and interleukine-6 (IL-6) in kidney homogenate were quantified using ELISA kits (cat RTFI01177 and cat RTEB1811, Assay Genie, London, UK). Malondialdehyde (MDA) (lipid peroxides), as well as the levels of total superoxide dismutase (SOD), total glutathione (GSH), glutathione peroxidase (GPx), catalase (CAT), and heme-oxygenase-1 (HO-1) levels in renal homogenate, were assessed by ELISA kits (Cat # MBS268427, MyBioSource, CA, USA, cat RTFI00215, Assay Genie, London, UK, RTEB0206, Assay Genie, London, UK and cat RTEB1811, Assay Genie, London, UK, Cat, MBS726781, MyBio-Source, CA, USA, and cat Ab279414, Abcam, Cambridge, UK). The levels of the Nrf2 and NF-κB in the nuclear and cytoplasmic fractions were quantified using ELISA kits (cat MBS752046 and cat MBS453975, MyBiosources, CA, USA). The cytoplasmic Keap-1 amounts were measured using an ELISA kit (cat MBS7218529, MyBiosources, CA, USA). All kits were rat-specific, and measurements were performed for all experimental groups (8 rats/group).

2.9. Biochemical measurements of apoptotic markers

The levels of the anti-apoptotic protein and Bcl2 were determined in the frozen homogenates by ELISA (Cat. MBS2881713, MyBiosources, CA, USA). Total levels of the apoptotic markers, cytochrome-c, Bax, and caspase-3 in renal homogenates were also measured by ELISA (Cat. MBS9304546, Cat. MBS93566,7 and Cat. MBS018987 MyBiosources, CA, USA, respectively). All kits were rat-specific, and analyses were performed in duplicate for n = 8 rats/group.

2.10. Assay of the intracellular ATP levels and mtPTP

ATP levels were measured in all samples using a colorimetric kit (Cat KA0806, Abnova, TX, USA). The opening of the mitochondrial permeability transition pore potential (mtPTP) was assessed using

the method described in the literature (Kavazis, 2009; Eid, 2021). The basic concept behind this approach is the finding that mitochondrial mTPT, which high Ca2+ causes, is prompted by oxidative stress. In brief, mitochondria from all frozen kidney tissues were separated using a mitochondria isolation kit (ab110168, Abcam, London, UK). The detached mitochondria were added to a special respiratory medium made up of 71 mM sucrose, 215 mM mannitol, 5 mM succinate, and 3 mM HEPES, which was then activated with 75 μM *tert*-butyl hydroperoxide and 400 μM CaCl₂ solutions. The decrease in absorbance due to mitochondria swelling was measured over 15 min at 540 nm. The maximum reduction in absorbance (Vmax) and the time to reach V_{max} were calculated as a function of mtPTP and increased mitochondria swelling, damage, and permeability.

2.11. Real-time polymerase chain reaction (q-PCR)

The primer pair sequences used for the q-PCR reaction are displayed in Table 1. Total RNA was extracted using a commercial kit (Cat 74004; Qiagen, Germany). The first-strand cDNA was created using a commercial cDNA synthesis kit (Cat K1621, The Thromo-Fisher kit). The amplification procedure was carried out in a CFX96 PCR machine using the Ssofast Evergreen Supermix kit as instructed by the manufacturer (Cat 172–5200, BioRad, USA). The amplification reactions were set as follows: (1) heating (1 cycle/98 °C/30 s), (2) denaturation (40 cycles/98 °C/5 s), (3) annealing (40 cycles/60 °C/5 s), and (4) melting (1 cycle/95 °C/5 s/step). After normalization with the reference gene (β-actin) using the 2ᐞᐞCT approach, the relative mRNA expression of each target gene was shown.

2.12. Western blotting

Frozen kidneys were homogenized in radioimmunoassay (RIPA) buffer (Cat 89901, ThermoFisher, USA). The Pierce™ BCA Protein Assay Kit (Cat. 23225, ThermoFisher, USA) was used to assess the total protein concentrations in samples. SDS-PAGE was used to separate equal quantities of each sample after proteins were diluted in the loading buffer. The proteins were then transferred to nitrocellulose membranes, blocked with 5% skimmed milk, and incubated with primary antibodies against Nrtf2 (Cat. 365949, 61 kDa, 1:1000, Santa Cruz Biotechnology, USA), cleaved caspase-3 (Cat. 9661, 19 kDa, 1:1000, Cell signaling Technology, USA), Keap-1 (Cat. 365626, 1:1000, Santa Cruz Biotechnology, USA, and β-actin (Cat. 3700, 45 kD, 1:1000). The membranes were then treated with the corresponding secondary antibodies and incubated with West pico PLUS chemiluminescence substrate (Cat # 34580, ThermoFisher, USA) for 5 min. The C-Di Git blot scanner was used to scan and examine the generated bands. The TBST buffer was used to wash three times every ten min in between each stage. All antibodies, as well as the skimmed milk, were diluted in the TBST buffer. Incubations with the primary or sec-

ondary antibodies were performed at room temperature for 2 h and with continuous shaking. All target proteins were normalized against β-actin.

2.13. Histopathological assessment

For 24 h, kidney sections were preserved in 10% buffered formalin. After being rehydrated in ethanol at progressively higher concentrations, tissues were cleaned with xylene. Following paraffin wax coating, the tissues were cut into 5 μm sections using a microtome. The tissue-sliced sections were stained with hematoxylin and eosin (HE) for the morphological tests. A light microscope with 200x magnification was used to take morphological images.

2.14. Statistical analysis

A one-way ANOVA was used to analyze all the data using GraphPad Prism software. Utilizing the Kolmogorov-Smirnov test, normality was evaluated. Tukey's test was used as a post hoc analysis to compare the various groups. At p < 0.05, data were deemed to be statistically different.
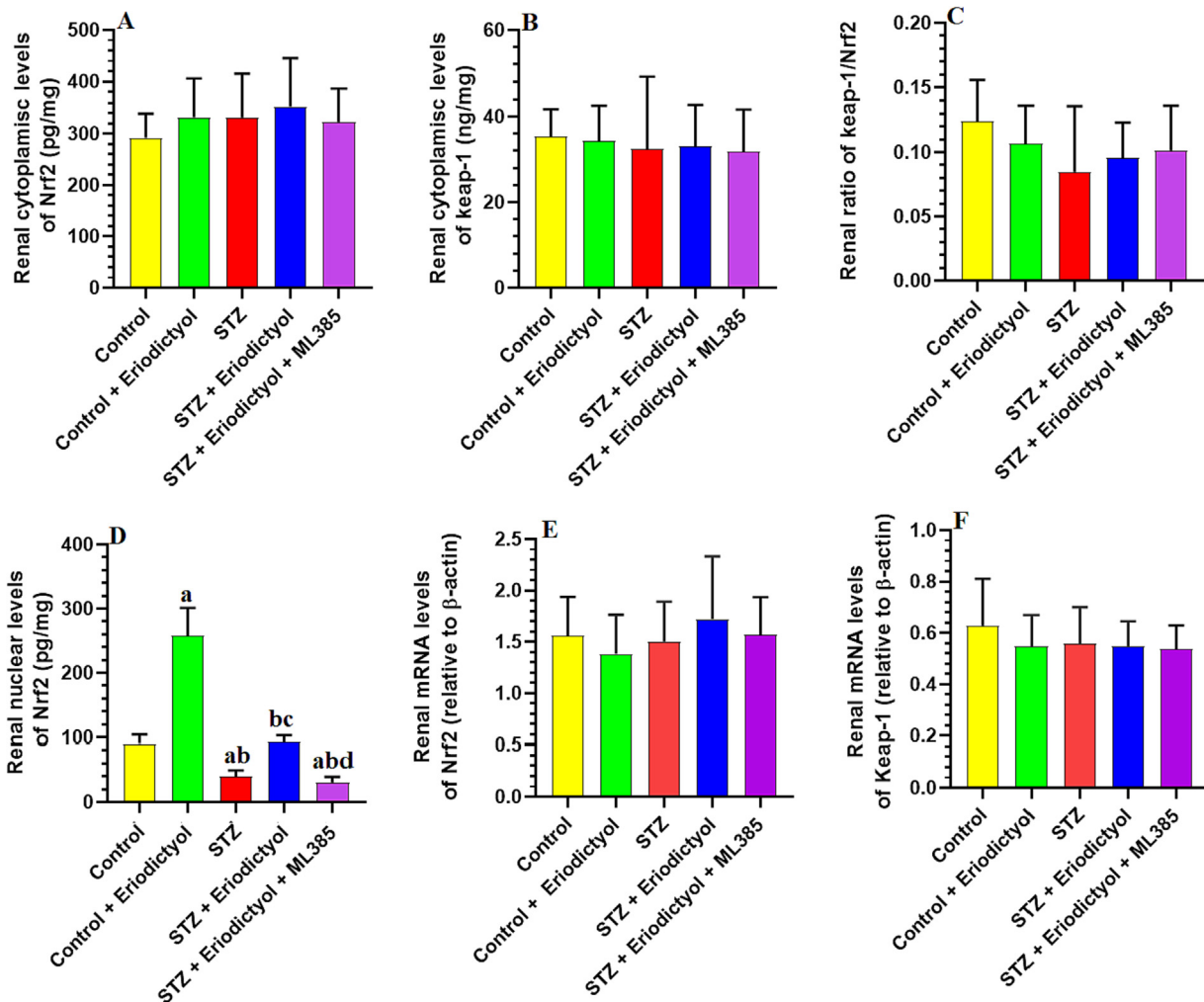
3. Results

3.1. Eriodictyol activates Nrf2 in the kidneys of STZ-Diabetic Rats, independent of modulating Nrf2 and Keap-1 expression

We found no significant difference in expression levels of the kidney's mRNA or total cytoplasmic Nrf2 in any tested rat group *(p > 0.05)* (Fig. 1). In addition, total cytoplasmic protein levels of Nrf2 and Keap-1 were not significantly different in the kidneys of any of the studied experimental groups *(p > 0.05)* (Fig. 1). On the other hand, the total nuclear Nrf2 expression levels, which were measured by ELISA or western blotting, were significantly lower in the kidneys of the STZ-treated group than in the control group *(p < 0.001)* (Fig. 1). The kidneys of eriodictyol- and STZ + eriodictyol-treated rats revealed a rise in the nuclear expression levels of Nrf2 compared to the control or STZ-model rat groups. We did not notice significant variations in the levels of nuclear protein Nrf2 in the STZ-diabetic group compared with the STZ + eriodictyol + ML385-treated group *(p > 0.05)* (Fig. 1).

3.2. Eriodictyol has an Nrf2-Dependent hypolipidemic effect but lacks any hypoglycemic properties in STZ-Diabetic rats

Fasting plasma glucose and insulin quantities increased significantly in STZ-treated rats, while the final body weight was significantly decreased compared to control non-diabetic rats *(p < 0.0001)* (Table 2). As can be seen in Table 2, STZ, STZ + eriodictyol, and STZ + eriodictyol + ML385 rat groups had insignificantly varied records of final body weights, fasting plasma glucose, or insulin levels *(p > 0.05)*. On the other hand, in comparison to the control, STZ-treated rats had fasting TGs, CHOL, FFAs, LDL-c, and ox-LDL-c levels significantly higher in STZ-treated rats, in contrast to significantly lower levels in eriodictyol-treated rats *(p < 0.01)* (Table 2). Furthermore, compared to the STZ model group, the amounts of these biochemical markers were significantly lower in STZ + eriodictyol-treated rats *(p < 0.001)* (Table 2). When compared to control rats, the levels of these biomarkers were all significantly higher in the STZ + eriodictyol + ML385-treated rats *(p < 0.05)*, but they were statistically indifferent when compared with STZ-treated rats *(p > 0.05)* (Table 2).

Table 1
Primers are used in the q-PCR reaction.

Gene	Primers (5′→3′)	Accession #	BP
Keap1	F: CTTCGGGGAGGA GGAGTTCT R: CGTTCAGATCATCGCGGCTG	NM_057152.2	132
Nrf2	F: -AAAATCATTAACCTCCCTGTTGAT R: CGGCGACTTTATTCTTACCTCTC	NM_031789	118
NF-κB	F: GTGCAGAAAGAAGACATTGAGGTG R: AGGCTAGGGTCAGCGTATGG	XM_342346.4	176
B-actin	F: GACCTCTATGCCAACACAGT R: CACCAATCCACACAGAGTAC	NM_031144	154

Fig. 1. Cytoplasmic levels of Nrf2 and keap-1 (A, B), the cytoplasmic ratio of keep-1/Nrf2 (C), nuclear levels of Nrf2 (D), and mRNA levels of Nrf2 (E) and keap-1 (F) in the kidneys of all groups of rats. Data are presented as means ± SD for n = 8 rats/group. Significance difference was considered if $p < 0.05$. (a): significantly differed with the control non-diabetic group; (b): significantly differed with the Eriodictyol-treated group; (c): significantly differed with STZ-treated diabetic rats; (d): significantly differed with STZ + Eriodictyol-treated group. ML385: a selective Nrf2 inhibitor.

Table 2
Final body weights, fasting plasma glucose, insulin, and serum lipid profile in all groups of rats.

		Control	Eriodictyol	STZ	STZ + Eriodictyol	STZ + Eriodictyol + ML385
Plasma	Final body weight	422.3 ± 33.7	421.5 ± 31.2	319.1 ± 25.4 [ab]	322.4 ± 24.9 [ab]	321 ± 29.2 [ab]
	Glucose (mg/dL)	112.3 ± 8.6	108.6 ± 9.4	320.1 ± 22.7 [ab]	306 ± 33.1 [abc]	311.8 ± 25.4 [ab]
	Insulin (ng/mL)	3.9 ± 0.52	4.1 ± 0.64	1.7 ± 0.17 [ab]	1.92 ± 0.14 [abc]	1.6 ± 0.22 [abd]
Serum	TGs (mg/dL)	84.5 ± 7.4	69.5 ± 5.9 [a]	192.2 ± 16.7 [ab]	101 ± 9.5 [abc]	203 ± 19.4 [abd]
	CHOL (mg/dL)	77.5 ± 6.5	55.5 ± 6.6 [a]	154.4 ± 12.3 [ab]	88.5 ± 8.4 [abc]	163.3 ± 14.3 [abd]
	LDL-c (mg/dL)	33.5 ± 4.9	22.5 ± 4.1 [a]	84.5 ± 6.9 [ab]	46.4 ± 4.3 [abc]	89.3 ± 8.6 [abd]
	FFAs (μmol/mg)	284.5 ± 22.5	266.3 ± 21.4 [a]	565.4 ± 47.6 [ab]	538 ± 55.6 [ab]	565.3 ± 61.4 [abd]
	Ox-LDL-c (ng/mL)	22.4 ± 2.8	15.4 ± 1.6 [a]	78.5 ± 6.3 [ab]	34.3 ± 3.2 [abc]	84.3 ± 7.5 [abd]

Data are presented as means ± SD for n = 8 rats/group. Significance difference was considered if $p < 0.05$. (a): significantly differed with the control non-diabetic group; (b): significantly differed with the Eriodictyol-treated group; (c): significantly differed with STZ-treated diabetic rats; (d): significantly differed with STZ + Eriodictyol-treated group. ML385: a selective Nrf2 inhibitor.

3.3. Eriodictyol improves STZ-Diabetic rat kidney function by activating Nrf2

Compared to control rats, STZ-treated rats had significantly higher serum Cr and urinary albumin quantities, whereas serum albumin and urinary Cr amounts were significantly lower ($p < 0.001$) (Table 3). In addition, urine volume, as well as urinary levels of KIM-1, MCP-1, and nephrin were significantly higher in rats treated with STZ if compared to untreated rats ($p < 0.01$). None of these biochemical parameters were found to be significantly different when the control rats and the rats treated with eriodictyol were compared ($p > 0.05$) (Table 3). Moreover, serum Cr levels, urine volume, and levels of albumin, KIM-1, MCP-1, and nephrin in urine were significantly reduced, and serum albumin amounts were significantly increased in rats treated with STZ + eriodictyol in comparison with rats treated with STZ alone ($p < 0.01$) (Table 3).

Table 3
Markers of kidney function in all groups of rats.

		Control	Eriodictyol	STZ	STZ + Eriodictyol	STZ + Eriodictyol + ML385
Serum	Urea (mg/dL)	5.2 ± 0.57	5.8 ± 0.72	33.5 ± 4.1 [ab]	6.3 ± 0.74[c]	30.2 ± 3.6 [abd]
	Creatinine (mg/dL)	0.63 ± 0.05	0.61 ± 0.04	1.8 ± 0.0.23 [ab]	0.71 ± 0.12[c]	2.9 ± 0.41 [abd]
Urine	Volume (ml)	11.4 ± 2.4	10.9 ± 1.7	17.5 ± 2.1 [ab]	10.4 ± 2.9[c]	18.5 ± 2.4 [abd]
	Albumin (µg/dL)	22.5 ± 1.7	25.4 ± 3.8	62.3 ± 5.7 [ab]	31.3 ± 3.5 [abc]	68.4 ± 6.3 [abd]
	Creatinine (µg/dL)	65.7 ± 5.6	62.3 ± 6.3	22.8 ± 1.9 [ab]	51.3 ± 3.9 [abc]	25.1 ± 2.4 [abd]
	MCP-1 (pg/mL)	178.3 ± 12.8	165.3 ± 15.7	438.2 ± 37.5 [ab]	235.1 ± 19.2 [abc]	458.1 ± 43.2 [abd]
	KIM-1 (ng/mL)	1.56 ± 0.2	1.68 ± 0.2	4.65 ± 0.5 [ab]	2.1 ± 0.4 [abc]	4.30 ± 0.6 [bd]
	Nephrine (ng/mL)	5.23 ± 0.4	4.88 ± 0.6	14.3 ± 1.8 [ab]	6.7 ± 0.8 [abc]	15.3 ± 1.8 [bd]

Data are presented as means ± SD for n = 8 rats/group. Significance difference was considered if $p < 0.05$. (a): significantly differed with the control non-diabetic group; (b): significantly differed with the Eriodictyol-treated group; (c): significantly differed with STZ-treated diabetic rats; (d): significantly differed with STZ + Eriodictyol-treated group. ML385: a selective Nrf2 inhibitor.

The opposite was true when comparing these biomarkers in rats treated with STZ + eriodictyol + ML385 versus those treated with STZ + eriodictyol. Compared to STZ model rats, STZ + eriodictyol + ML-385 treated group revealed no significant changes in the urine volume, as well as these biomarker quantities in serum and urine ($p > 0.05$) (Table 3).

3.4. Eriodictyol renal antioxidant potential in STZ-Diabetic kidneys via activating Nrf2

In comparison to control rats, STZ-diabetic rats exerted significantly higher levels of MDA in kidney tissues and significantly lower levels of SOD, GSH, CAT, GPx, and HO-1 in blood serum ($p < 0.0001$) (Fig. 2). The control + eriodictyol- and STZ + eriodictyol-treated rats had significantly lower renal MDA levels as well as significantly elevated levels of GSH, SOD, CAT, GPx, and HO-1 when compared to the control or STZ-treated rats ($p < 0.0001$) (Fig. 2). The MDA amounts in the rat group treated with STZ + eriodictyol + ML385 were significantly elevated, while the levels of the aforementioned antioxidants were significantly diminished when compared to STZ-prompted diabetic rats ($p < 0.01$). The levels of all these biochemical endpoints did not vary significantly between the STZ-treated rats and STZ + eriodictyol + ML385-treated rats ($p > 0.05$) (Fig. 2).

3.5. Eriodictyol suppresses renal inflammation in STZ-Diabetic kidneys by activating Nrf2

As compared to control rats, the rat kidneys treated with STZ had significantly higher levels of NF-κB in the cytoplasm and nucleus and total levels of IL-6 and TNF-α ($p < 0.001$) (Fig. 3). All these inflammatory markers did not vary significantly between the control and the eriodictyol-treated rats or between the STZ and STZ + eriodictyol + ML385-treated rats ($p > 0.05$) (Fig. 3). In comparison to the STZ-diabetic rats or the STZ + eriodictyol + ML385-treated rats, the STZ + eriodictyol-treated rats had significantly lower levels of NF-κB in the cytoplasm and nucleus and total levels of TNF-α and IL-6 ($p < 0.001$) (Fig. 3).

3.6. Eriodictyol inhibits renal inflammation in STZ-Diabetic kidneys by activating Nrf2

No significant changes in the total renal levels of caspase-3, Bcl2, and Bax, as well as in the levels of cytoplasmic cytochrome-c were seen between the control rats and those control which were treated with eriodictyol ($p > 0.05$) (Fig. 4). The Bcl2 expression levels decreased significantly, but the total levels of cytoplasmic cytochrome-c, Bax, and caspase-3 increased significantly in the STZ-treated rat kidneys compared to the control rats ($p<0.001$). The levels of all of these biomarkers were reversed in the rat kidneys treated with STZ + eriodictyol when compared to STZ-

diabetic rats (Fig. 4). As compared to STZ-model rats, the rats treated with STZ + eriodictyol + ML385 showed no significant changes in the expression levels of cytoplasmic cytochrome-c, caspase-3, Bcl2, and Bax ($p > 0.05$) (Fig. 4).

### 3.7. Eriodictyol improves kidney mitochondria function in STZ-Diabetic rats activating Nrf2

There were no significant differences in the ATP amount or the decline in absorbance (V_{max}), which is an indicator of mTPT opening, between the control rats and the rats treated with eriodictyol ($p > 0.05$) (Table 4). A significant drop in the levels of ATP paralleled with a significant rise in the reduction in absorbance (Vmax), was seen in the mitochondria of STZ-treated rats ($p < 0.0001$) (Table 4). The levels of all of these biochemical indicators were reversed in the rats treated with STZ + eriodictyol when compared with those in STZ-diabetic rats ($p < 0.001$) (Table 4). However, the ATP amounts dropped significantly, while Vmax values rose significantly in the rat mitochondria after STZ + eriodictyol + ML350 treatment compared to STZ + eriodictyol treatment ($p < 0.05$). There were no significant alterations in the ATP levels and Vmax values between the STZ and STZ + eriodictyol + Ml385-treated rats ($p > 0.05$) (Table 4).

3.8. Eriodictyol improves kidney architecture in STZ-Diabetic rats activating Nrf2

The control and eriodictyol-treated rat kidneys were characterized by normal histological appearances like proximal convoluted tubules (PCTs), distal convoluted tubules, normal glomeruli, glomerular membrane, and glomerular capillaries (Fig. 5A, B). Kidneys from STZ-treated rats revealed reduced glomerular mass, elevated infiltration of immune cells, and damaged glomerular membrane, PCTs, and DCTs (Fig. 5C, D). The STZ + eriodictyol-treated animal kidneys demonstrated substantial structural recovery in the majority of PCTs and DCTs, with no signs of immune infiltration and normal glomerular membrane and mass (Fig. 5E). The kidney sections obtained from STZ + eriodictyol + ML385-treated rats exhibited similar pathological alterations to those found in STZ-diabetic kidneys (Fig. 5F).

4. Discussion

In this study, we provide the first in vivo evidence in the literature confirming the preventive impact of eriodictyol against DN in rats. Herein, the findings of this study, which used the STZ diabetic rat model, demonstrate that selective activation of Nrf2 is a crucial mechanism behind the anti-inflammatory, antioxidant, and anti-apoptotic renoprotection of eriodictyol. In addition, this effect was independent of modeling glucose or insulin levels but associated with the Nrf2-mediated anti-hyperlipidemia effect. Fur-
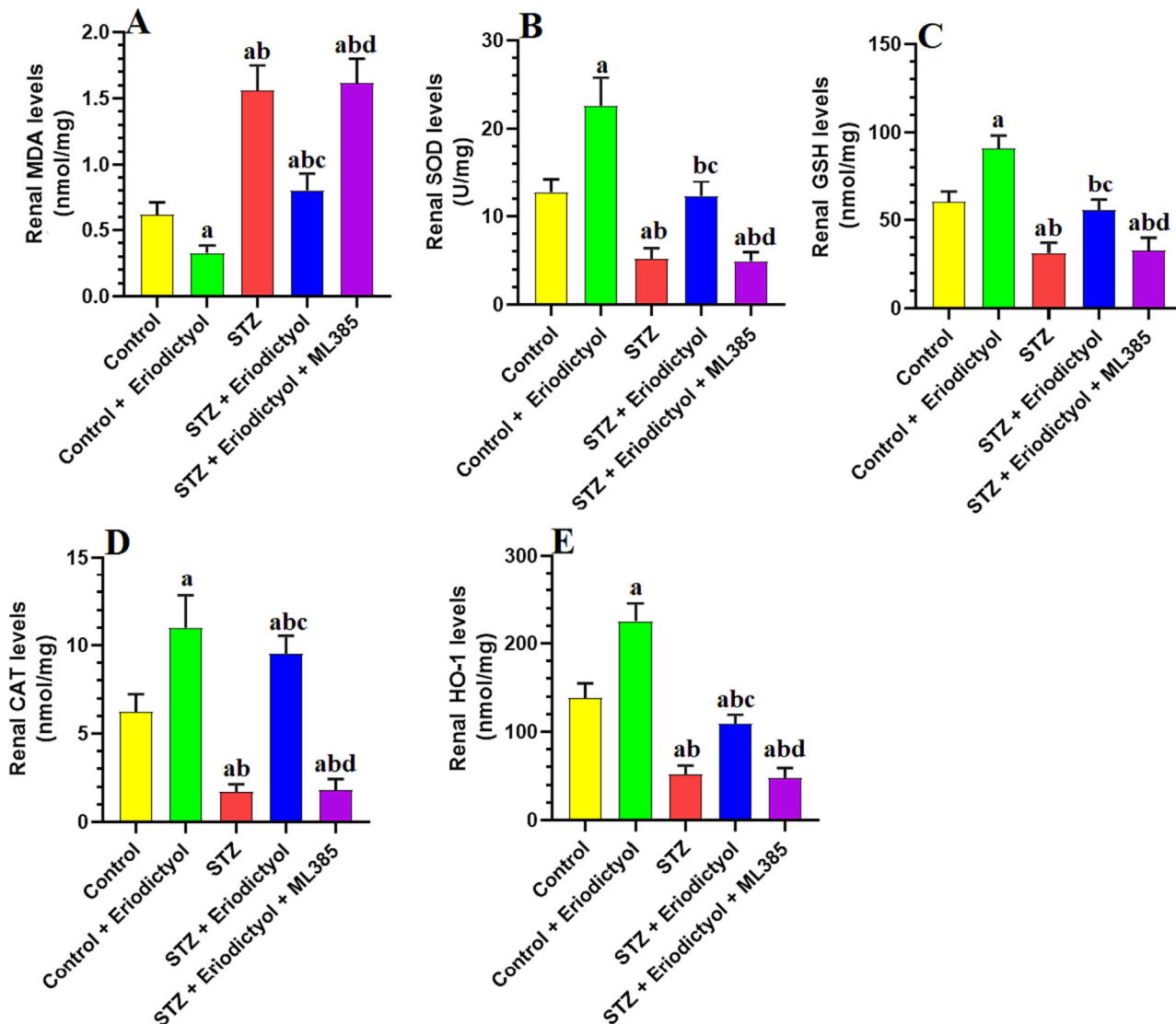
Fig. 2. Total levels of malondialdehyde (MDA) (A), superoxide dismutase (SOD) (B), total glutathione (GSH) (C), catalase (CAT) (D), and heme-oxygenase-1 (HO-1) (E) in the kidneys of all groups of rats. Data are presented as means ± SD for n = 8 rats/group. Significance difference was considered if $p < 0.05$. (a): significantly differed with the control non-diabetic group; (b): significantly differed with the Eriodictyol-treated group; (c): significantly differed with STZ-treated diabetic rats; (d): significantly differed with STZ + Eriodictyol-treated group. ML385: a selective Nrf2 inhibitor.

thermore, the study's remaining results also imply that eriodictyol's capability to change how keap-1 and Nrf2 interact may be the cause of this Nrf2 activation in the kidneys.

The benefit of STZ usage to induce insulin deficiency has been confirmed in numerous studies to produce similar clinical symptoms to those seen in autoimmune T1DM in rats and diabetic patients (Graham et al., 2011; Damasceno et al., 2014). The chemotherapeutic drug STZ, a glucosamine-nitrosourea substance produced by Streptomyces achromogenes, is commonly used to treat pancreatic β-cell carcinoma (Damasceno et al., 2014). STZ is extremely harmful to the pancreatic β cells owing to its preferential entry and accretion through the GLUT2 receptors (Dufrane et al., 2006; Lenzen, 2008). The pancreatic toxicity of STZ depends on the treatment dose, where higher doses (>55 mg/kg) act by DNA alkylating, whereas the lower doses induce cell inflammation and oxidative stress (Paik et al., 1980; Graham et al., 2011; Damasceno et al., 2014). Under both conditions, STZ leads to sustained hyperglycemia, which promotes renal hemodynamic, functional, and structural abnormalities, including reduced GFR, microalbuminuria, low Cr excretion, tubular and glomerular

degeneration, and interstitial fibrosis (Graham et al., 2011). High amounts of glycated hemoglobin (HbA1c) and the existence of microalbuminuria and low Cr excretion are valid diagnostic for evaluating kidney function in DN (Little et al., 2013; Selby and Taal et al., 2020). A spike in HbA1c of just 1% raises the possibility of developing diabetic microvascular problems by 40%, whereas HbA1c levels above 7% positively correlate with DN and microalbuminuria in people with diabetic kidney disease (Khan et al., 2020). Even though no definite treatment is still available to treat DN, controlling blood glucose levels prevents the development of microalbuminuria and renal injury and delays the progression to ESRD (Sampanis, 2008).

The significantly higher amounts of glucose, insulin, and HbA1C, as well as the decreased Cr clearance, the higher urinary excretion of albumin, and the pathological evidence of the damage to the renal glomerular and tubular cells in STZ-treated rats, validated our animal model and supported all the aforementioned studies. On the other hand, the reversal of all these effects without significant decline in fasting glucose, insulin, or HbA1c quantities in STZ + eriodictyol-treated rats suggests that the nephroprotective
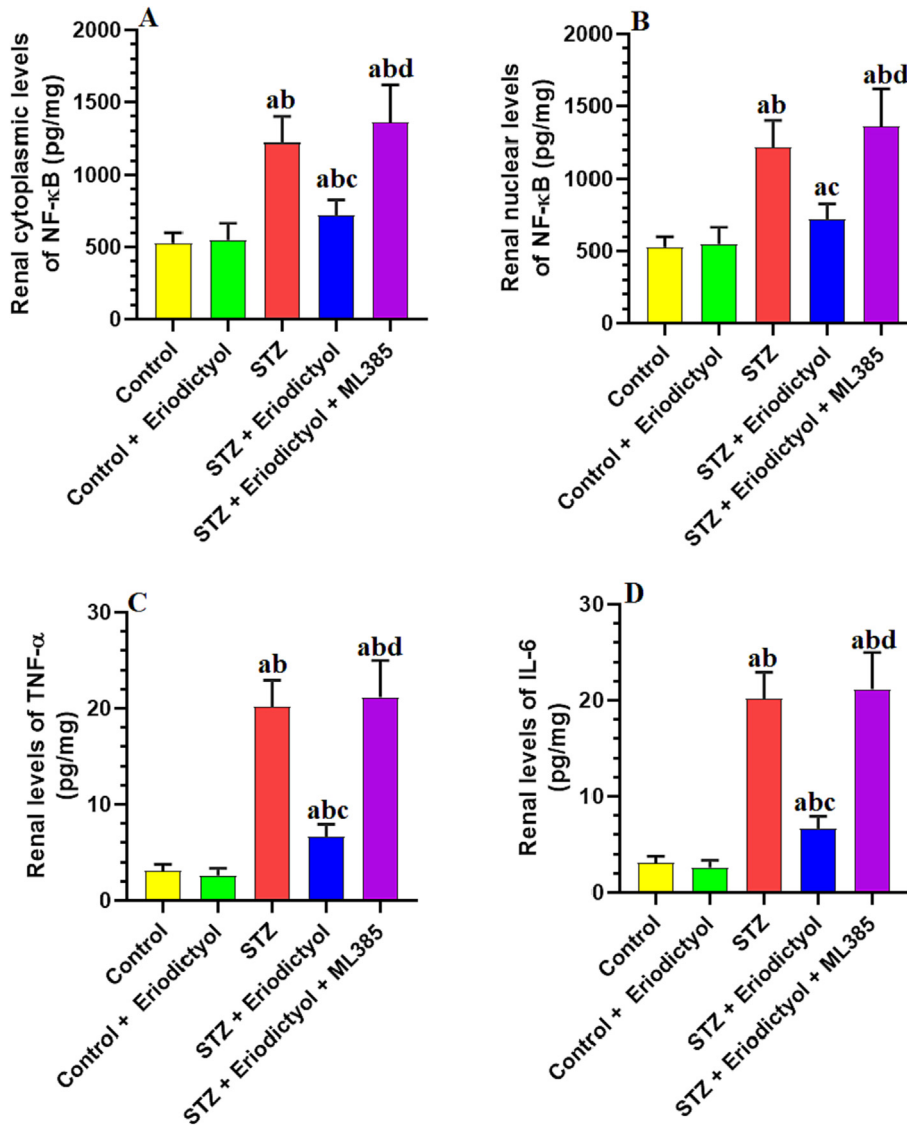
Fig. 3. Cytoplasmic and nuclear levels of NF-κB (A, B), as well as total levels of tumor necrosis factor-alpha (TNF-α) (C) and interleukine-6 (IL-6) (D) in the kidneys of all groups of rats. Data are presented as means ± SD for n = 8 rats/group. Significance difference was considered if p < 0.05. (a): significantly differed with the control non-diabetic group; (b): significantly differed with the Eriodictyol-treated group; (c): significantly differed with STZ-treated diabetic rats; (d): significantly differed with STZ + Eriodictyol-treated group. ML385: a selective Nrf2 inhibitor.

effect of this drug did not depend on modulating peripheral or hepatic glucose homeostasis or the production and excretion of insulin from the pancreas. Therefore, it seems reasonable that the effect of eriodictyol is through its effect on the kidneys themselves. Few studies have been conducted to examine the hypoglycemic effect. An in vivo study conducted by Zhang et al. (2012) has discovered that eriodictyol increases muscular and adipose tissue glucose uptake and, therefore, can increase peripheral insulin sensitivity (Zhang et al., 2012). Similar results were also confirmed in vivo in HFD-fed rats (Kwon and Choi, 2019). These findings contradict our results, and this discrepancy with our data could be explained by the differences between the animal models used to stimulate T1DM and T2DM (i.e., STZ vs. HFD).

On the other hand, our data show that eriodictyol has potent anti-inflammatory, antioxidant, and anti-apoptotic impacts on the kidneys of STZ-treated rats, which underlie its nephroprotective effect. During the last decades, several experimental, clinical, and observational studies have shown the important role of oxidative stress, inflammation, or apoptosis in mediating DN by acting

collaboratively to induce an endless activation loop (Jing et al., 2013). Interestingly, a consensus is showing that hyperglycemia-derived ROS are the major indispensable upstream regulator that induces DN by promoting the activation of diverse inflammatory, fibrotic, hypertrophic, and apoptotic pathways (Kashihara et al., 2010; Jha et al., 2016). In DM, hyperglycemia generates massive amounts of ROS from different resources, including glucose-autoxidation, induction of advanced-glycation products (AGEs), impairing oxidative phosphorylation and mitochondria function, activating of NADPH oxidase, and overwhelming the enzymatic and non-enzymatic cellular antioxidants (Ali et al., 2018; Wei and Szeto, 2019; Matoba et al., 2020; Sugahara et al., 2021; Hung et al., 2021). The damaging effects of ROS on the kidneys are well-reported in several reports.

Within this view, ROS damages the renal cells by promoting oxidative DNA, protein, and lipid peroxidation (Mahmoodnia et al., 2017). Furthermore, ROS can cause mitochondria-mediated cell death and enhance the release of cytochrome-c from the mitochondria by activating the p53/Bax pathways and downregulating
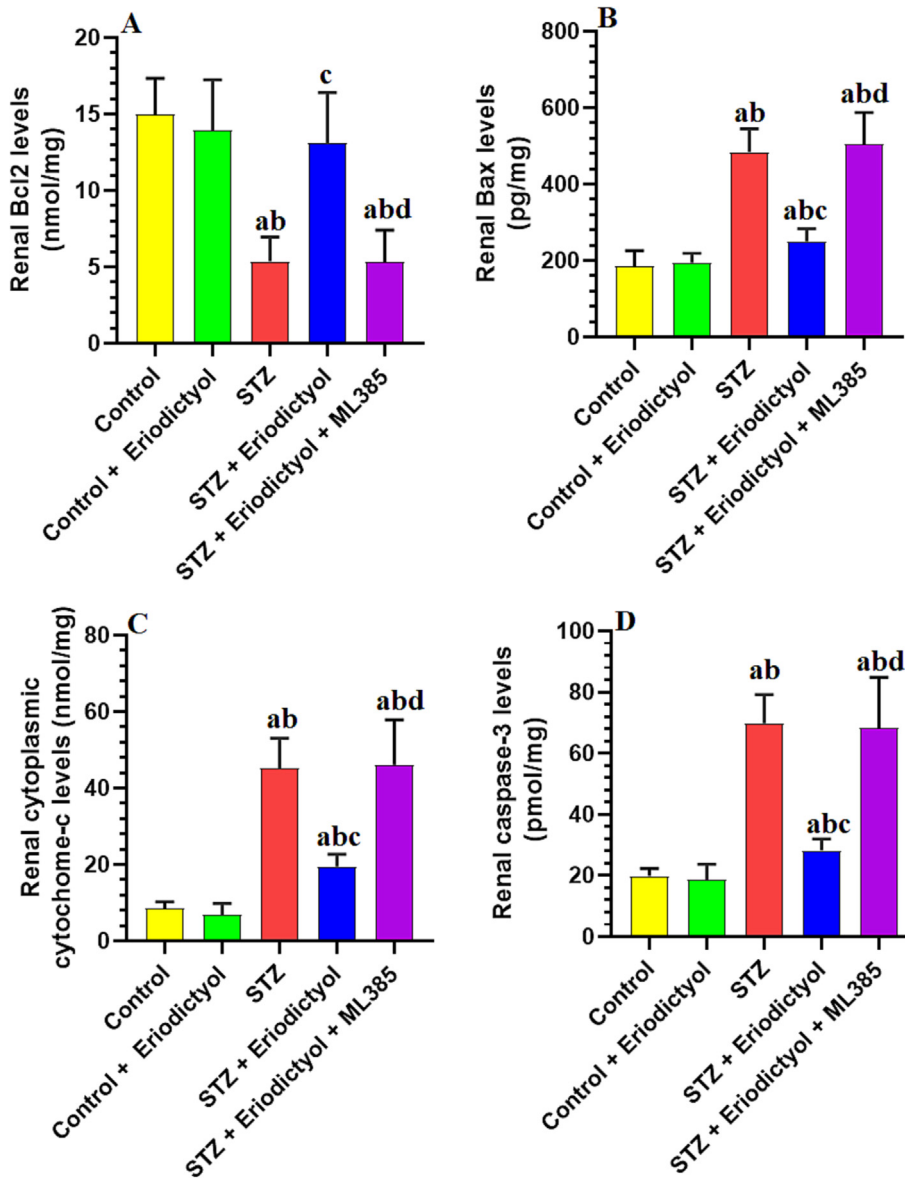
Fig. 4. Total levels of Bcl2 (A), Bax (B), caspase-3 (C), and cytoplasmic levels of cytochrome-c (D) in the kidneys of all groups of rats. Data are presented as means ± SD for n = 8 rats/group. Significance difference was considered if $p < 0.05$. (a): significantly differed with the control non-diabetic group; (b): significantly differed with the Eriodictyol-treated group; (c): significantly differed with STZ-treated diabetic rats; (d): significantly differed with STZ + Eriodictyol-treated group. ML385: a selective Nrf2 inhibitor.

Table 4
Levels of ATP and mitochondria permeability transition pore potential (mtPTP) opening in the isolated mitochondria.

	Control	Eriodictyol	STZ	STZ + Eriodictyol	STZ + Eriodictyol + ML385
ATP levels (nmol/mg)	33.6 ± 3.1	31.7 ± 2.4	14.6 ± 1.2 [ab]	29.5 ± 3.6[c]	15.2 ± 1.8 [abd]
mtTPTopening V_{max} (ΔABS/min)	0.45 ± 0.05	0.51 ± 0.04[a]	0.92 ± 0.1 [ab]	0.53 ± 0.05[c]	0.84 ± 0.07 [abd]

Data are presented as means ± SD for n = 8 rats/group. Significance difference was considered if $p < 0.05$. (a): significantly differed with the control non-diabetic group; (b): significantly differed with the Eriodictyol-treated group; (c): significantly differed with STZ-treated diabetic rats; (d): significantly differed with STZ + Eriodictyol-treated group. ML385: a selective Nrf2 inhibitor.

the level of Bcl2 expression (Mahmoodnia et al., 2017; Ali et al., 2018). Also, ROS-induce renal inflammation and increases the synthesis of diverse inflammatory adhesive molecules, cytokines, and chemokines via direct activation of inflammasome-3 and NF-κB (Matoba et al., 2019). As a discontinuous loop, NF-κB, IL-6, and TNF-α further exaggerate the generation of ROS, leading to a sustained state of oxidative stress, inflammation, and apoptosis (Pichler et al., 2017; Alicic et al., 2018).

In this research, the kidneys of STZ-diabetic rats showed greater amounts of IL-6 and TNF-α, as well as higher nuclear generation of NF-κB in the kidneys. They also had reduced ATP levels and increased mTPT opening, which indicates mitochondria damage and dysfunction. Also, STZ-diabetic rat's urine samples demonstrated higher levels of MDA biochemical indicators of lipid peroxidation. These findings agree with those of earlier research on diabetic individuals and animals (Goodarzi et al., 2010; Khaki
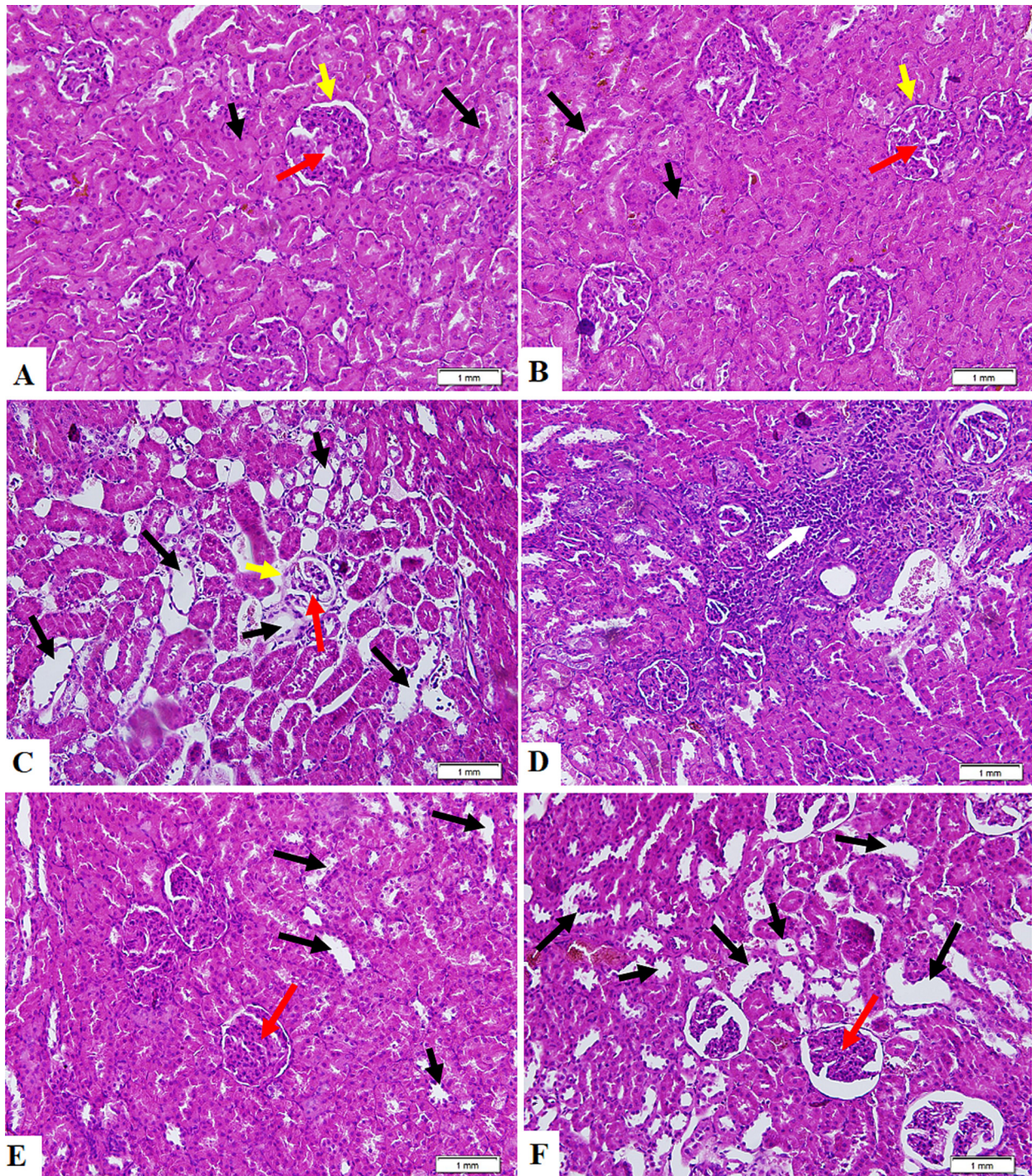
Fig. 5. Histology evaluation of all kidney sections obtained from all groups of rats as stained by hematoxylin and eosin (H&E) staining. (A, B): were taken from control rat and eriodictyol-treated rats, respectively, and showed normal Bowman's capsule containing intact glomeruli and glomerular membrane (yellow arrow), as well as intact distal convoluted tubules (DCTs) (Long black arrow) and proximal convoluted tubules (PCTs) (short black arrow). (C, D): were taken from STZ-diabetic rats and showed apparent damage and shrinkage in the glomerulus capillaries (red arrow) and damaged glomerular membrane (red arrow). Most PCTs and DCTs were damaged (short and black arrows, respectively), associated with increased inflammatory cell infiltration (white arrow). (E): was taken from STZ + eriodictyol-treated kidney and showed almost normal features in most fields, including intact glomeruli, glomerular membranes, PCTs, and DCTs. However, some DTCs and PCTs showed some damage but less than seen in the STZ group (long and short black arrows). (F): was taken from STZ + eriodictyol + ML385-treated kidney and showed similar pathological changes to those seen in group C (STZ-diabetic group).

et al., 2014; Mestry et al., 2017; Sanchez et al., 2018; Matoba et al., 2020; Vodošek Hojs et al., 2020; Shawki et al., 2021). In addition, the kidneys of STZ-rats had significantly lower amounts of GSH, CAT, GPx, SOD, and HO-1, which indicate an overall consumption of antioxidants due to the overproduction of ROS, conforming to the results of previous studies (Khaki et al., 2014; Gomathi et al., 2014; Chtourou et al., 2022). Furthermore, the mRNA levels of caspase-3 and Bax, as well as the cytoplasmic levels of cytochrome-c and protein expression of cleaved caspase-3 increased significantly, whereas the mRNA levels of Bcl2 reduced

significantly in the diabetic rat kidneys. Together, these findings support the involvement of oxidative stress, inflammation, and apoptosis in the pathogenesis of DN. Similar to these results, higher levels of AGEs were reported in diabetic kidneys and associated with increased ROS generation through bindings to their receptors (Hung et al., 2021). Furthermore, we have confirmed the contribution of oxidative stress and inflammation to DN by measuring other significant markers, including MCP1 nephrin, and KIM-1, which were also increased in the STZ-prompted diabetic rats' urine. Indeed, MCP-1 is a major inflammatory chemokine predictor of DN and is largely correlated with oxidative stress, inflammation, glomerular damage, tubular hypertrophy, necrosis, and apoptosis (Scurt et al., 2022). The increase in urinary levels of MCP-1 has been reported during the early stage of DN and is largely correlated with the higher expression of nephrin and KIM-1, two precise biomarkers for glomerular damage (Sampanis, 2008; Pichler et al., 2017; Siddiqui et al., 2020; Tuttle and Alicic 2021).

Eriodictyol administration significantly reduced the advancement of all the changes that happened in the kidneys of diabetic animals, demonstrating the substance's potent antioxidative and anti-inflammatory properties. Eriodictyol had no influence on the amounts of any of these indicators in the control rats' kidneys, but it considerably reduced the MDA levels and raised the levels of CAT, HO-1, GSH, SOD, and GPx, indicating its crucial role in upregulating the antioxidants in the renal cells. Therefore, these findings confirm the inhibitory action of eriodictyol on markers of inflammation and apoptosis, which is secondary to its antioxidant capability. Besides these findings, the data of this examination depicted novel, interesting evidence suggesting that Nrf2 activation in kidneys is a potential mechanism of action for the anti-inflammatory, antioxidant, and anti-apoptotic influences of eriodictyol. Indeed, treatment with eriodictyol significantly boosted the Nrf2 nuclear activation in the kidneys of the control rat group and diabetic rat group, which is consistent with the higher levels of all the above-mentioned antioxidant markers. However, ML385's suppression of Nrf2 eliminated all of eriodictyol's advantageous antioxidant, anti-inflammatory, and anti-apoptotic activities. Nrf2 is the most-known transcription factor that encourages the formation of SOD, CAT, HO-1, and GSH in the majority of mammalian cells (Baird and Yamamoto, 2020). In addition, Nrf2 inhibits the NF-κB activation by blocking the formation of ROS and augmenting the phosphorylation-mediated degeneration of IκBα, which normally stimulates the nuclear translocation and activation of NF-κB (Thimmulappa et al., 2006; Wardyn et al., 2015). Furthermore, Nrf2 is the prominent key factor in maintaining mitochondria structure, function, and homeostasis function and effectively increases ATP levels and counteracts the production of ROS by upregulating the uncoupling protein 3 (UCP3), improving FA oxidation, promoting mitophagy, stimulating PGC-1α-mediated mitochondria biosynthesis (Dinkova-Kostova and Abramov, 2015).

Supporting our data, the anti-inflammatory and antioxidant protective impacts of eriodictyol were reported in several studies of other animal models and were linked to the activation of the Nrf2 pathway. Indeed, eriodictyol inhibited the NF-κB activation and inflammatory damage caused by IL-1β in chondrocytes by stimulating the Nrf2/HO-1 pathway (Wang et al., 2018). This evidence also confirmed that the inhibitory impact of eriodictyol on NF-κB may be related to its stimulation of Nrf2. Similarly, it prevented LPS-induced lung damage and inflammatory cytokine expression in the macrophages by stimulating Nrf2 (Zhu et al., 2015). In addition, eriodictyol alleviated spinal cord injury in rats by Nrf2-dependent stimulation of GSH, SOD, and CAT and suppressing NF-κB (Mao et al., 2020). In the same line, eriodictyol prevented cisplatin-mediated nephropathy by activating the pathways of Nrf2/NF-κB and Nrf2/antioxidant (Li et al., 2016). Also, eriodictyol prevented apoptosis caused by ROS in cultured cardiac

and endothelial cells by activating the Nrf2 nuclear translocation and boosting its antioxidant transcriptional process (Lee et al., 2015; Li et al., 2016). Moreover, eriodictyol protected against cerebral ischemic injury and β-amyloid-induced oxidative apoptosis in cultured neurons and alleviated H_2O_2-induced oxidative damage in prostate cells. It also protects against oxidative damage to retinal cells (neuron-like PC12 cells) by activating the Nrf2/ARE/antioxidant signaling pathway (Jing et al., 2013; Lou et al., 2012; Jing et al., 2015). In the same line, eriodictyol prevented high glucose-mediated retinal ganglion cell (RGCs) damage by promoting the Nrf2/antioxidant axis and diminishing NF-κB (Lv et al., 2019). Also, eriodictyol inhibited the rise of mucin in the airway epithelial cells, the proliferation and metastasis of glioma cells, and the colitis caused by trinitrobenzene sulfonic acid (TNBS) in mice by inhibiting NF-κB signaling (Li et al., 2021; Hu et al., 2021; Yun et al., 2021). Further, research demonstrates that the therapeutic potential of eriodictyol is mainly due to the activation of Nrf2 (Deng et al., 2020).

Hyperlipidemia is another independent factor mediating DN (Schelling, 2022). Higher amounts of TGs, CHOL, LDL, and ox-LDL-c have been found in the serum of diabetic patients and rodents, which together coordinately promoted DN (Chen and Tseng, 2013; Kawanami et al., 2016; Hirano et al., 2022). Hypercholesterolemia exaggerates albuminuria in diabetic rats (Utsunomiya et al., 1995). On the contrary, lipid-lowering drugs improved glomerulosclerosis restored normal kidney function, and prevented microalbumin urea in diabetic patients and in Zucker rats, which are the best-known model of DM complicated with hyperlipidemia (Kasiske et al., 1988; Chen et al., 2005). Many mechanisms have been put forward to explain the crucial contribution of hyperlipidemia to renal damage (Hirano et al., 2022). On the other side, high TGs and LDL-c initiate renal inflammation and oxidative stress by activating the TG-rich lipoprotein receptors (TGRLs) (Gröne et al., 1990; Wheeler et al., 1991; Krämer et al., 1993; Quaschning et al., 1997; Hirano et al., 2022). These TGRLs are normally and highly expressed on the podocytes and can stimulate the formation of TNF-α, TGF-β1, and IL-6, thereby spiking ROS formation (Hirano et al., 2022). In addition, ox-LDL-c can stimulate the extracellular matrix protein expressions and MCP-1 formation in the mesangial cells, which in turn enhances macrophage infiltration and subsequently inflammation (Kamanna et al., 1996; Li and Mehta 2000). This could be the reason why the urine samples of the diabetic rats showed higher MCP-1 levels. Furthermore, diabetic kidneys of STZ-treated animals express high levels of Toll-like receptor (TLR) 4 and sterol regulatory element binding protein (SREBP)-1, which trigger NF-κB activation and the fatty acid synthesis genes' expression, respectively (Brown and Goldstein, 1997; Ishigaki et al., 2007; Mitrofanova et al., 2021). It's interesting to note that in SREBP-1-deficient mice, the advancement of DN is prevented (Ishigaki et al., 2007). A high-fat diet-fed TLR4-deficient mouse model has also been shown to mitigate the development of DN (Brown and Goldstein, 1997; Kuwabara et al., 2012). Also, the increased glycation of accumulated LDL-c in the kidneys was shown to be another mechanism for inducing renal damage, inflammation, and oxidative stress (Hirano et al., 2022).

Our findings also illustrate that the nephroprotective impact of eriodictyol involves a potent hypolipidemic effect. Within this context, eriodictyol treatment not only improved CHOL, TGs, FFAs, LDL-c, and ox-LDL-c quantities in the sera of STZ-prompted diabetic rats but also the sera of control rats too, suggesting an interesting hypolipidemic effect. Similar to our data, previous evidence has also shown that eriodictyol reduced the amounts of serum CHOL, free fatty acids, and TGs, and attenuated liver steatosis and lipid accumulation in rats fed a high-fat diet via decreasing the intestinal absorption of fat, suppressing de novo lipogenesis

through downregulating SREBP1 and downstream lipogenic genes, and activating fatty acid oxidation by stimulating PPARα (Kwon and Choi, 2019). However, we have further extended these data and confirmed that these effects are mainly regulated by activating the Nrf2 signaling pathways. Herein, treatment with ML385 completely abolished the hypolipidemic effect of eriodictyol and significantly increased CHOL, TGs, FFAs, LDL-c, and ox-LDL-c levels in the serum. Therefore, we could postulate that eriodictyol attenuates the impairment in circulatory lipids by activating Nrf2. Indeed, in addition, to stimulating antioxidant expression, Nrf2 can suppress hepatic CHOL and TGs by downregulating SREBP1, fatty acid synthase (FAS), and diacylglycerol acyltransferase-1 (Huang et al., 2010; Thornalley and Rabbani, 2012; da Silva Reis et al., 2016).

However, one major limitation in this study remains is that we still lack the precise mechanism by which eriodictyol stimulates Nrf2. According to the available literature, the activation of Nrf2 occurs via several mechanisms, including increasing Nrf2 release by modifying Keap-1 cysteine thiol residues, inducing oxidative stress, downregulation of Keap-1 expression, stimulating Nrf2 expression, inhibiting Nrf2 proteasome degradation, and reducing Nrf2 nuclear export (Wu et al., 2020). In our study, since eriodictyol showed no effect on the mRNA Nrf2 levels and the mRNA and protein expression levels of keap-1, these data suggest that eriodictyol may act by preventing keap-1 and Nrf2 from interacting. It could be possible that eriodictyol increased the transcriptional activity of Nrf2 by reducing its proteasome degradation and/or its nuclear export in the cytoplasm. However, the precise mechanism behind this can't be depicted based on these data and may require further examination.

In conclusion, the data of this study provide the first evidence for the protective effect of eriodictyol against T1DM-induced DN in rats. It also supports that this protection is mediated by antioxidant and anti-inflammatory effects, mainly due to the activation of Nrf2. This represents a window for future research at the preclinical and clinical levels.

Funding

Declaration of Competing Interest

The authors declare that they have no known competing financial interests or personal relationships that could have appeared to influence the work reported in this paper.

Acknowledgments

References

Ali, D., Tripathi, A., Al Ali, H., Shahi, Y., Mishra, K.K., Alarifi, S., Alkahtane, A.A., Manohardas, S., 2018. ROS-dependent Bax/Bcl2 and caspase 3 pathway-mediated apoptosis induced by zineb in human keratinocyte cells. Onco Targets Ther., 489–497

Alicic, R.Z., Johnson, E.J., Tuttle, K.R., 2018. Inflammatory mechanisms as new biomarkers and therapeutic targets for diabetic kidney disease. Adv. Chronic Kidney Dis. 25, 181–191.

Al-Waili, N., Al-Waili, H., Al-Waili, T., Salom, K., 2017. Natural antioxidants in the treatment and prevention of diabetic nephropathy; a potential approach that warrants clinical trials. Redox Rep. 22, 99–118.

Bai, J., Wang, Y., Zhu, X., Shi, J., 2019. Eriodictyol inhibits high glucose-induced extracellular matrix accumulation, oxidative stress, and inflammation in human glomerular mesangial cells. Phytother. Res. 33, 2775–2782.

Baird, L., Yamamoto, M., 2020. The molecular mechanisms regulating the KEAP1-NRF2 pathway. Mol. Cell Biol. 40. e00099-00020.

Bolignano, D., Cernaro, V., Gembillo, G., Baggetta, R., Buemi, M., D'Arrigo, G., 2017. Antioxidant agents for delaying diabetic kidney disease progression: a systematic review and meta-analysis. PLoS One 12, e0178699.

Brown, M.S., Goldstein, J.L., 1997. The SREBP pathway: regulation of cholesterol metabolism by proteolysis of a membrane-bound transcription factor. Cell 89, 331–340.

Bucolo, C., Leggio, G.M., Drago, F., Salomone, S., 2012. Eriodictyol prevents early retinal and plasma abnormalities in streptozotocin-induced diabetic rats. Biochem. Pharmacol. 84, 88–92.

Buranasudja, V., Muangnoi, C., Sanookpan, K., Halim, H., Sritularak, B., Rojsitthisak, P., 2022. Eriodictyol attenuates H2O2-Induced oxidative damage in human dermal fibroblasts through enhanced capacity of antioxidant machinery. Nutrients 14, 2553.

Chen, H.-C., Guh, J.-Y., Chang, J.-M., Hsieh, M.-C., Shin, S.-J., Lai, Y.-H., 2005. Role of lipid control in diabetic nephropathy. Kidney Int. 67, S60–S62.

Chen, Y.-J., Kong, L., Tang, Z.-Z., Zhang, Y.-M., Liu, Y., Wang, T.-Y., Liu, Y.-W., 2019. Hesperetin ameliorates diabetic nephropathy in rats by activating Nrf2/ARE/glyoxalase 1 pathway. Biomed. Pharmacother. 111, 1166–1175.

Chen, S.-C., Tseng, C.-H., 2013. Dyslipidemia, kidney disease, and cardiovascular disease in diabetic patients. Rev. Diabet. Stud. RDS. 10, 88. Kawanami, D., Matoba, K., Utsunomiya, K., 2016. Dyslipidemia in diabetic nephropathy. Ren. Replace. Ther. 2, 1–9.

Chtourou, Y., Morjen, M., Ammar, R., Mhiri, R., Jemaà, M., ELBini-Dhouib, I., Fetoui, H., Srairi-Abid, N., Marrakchi, N., Jebali, Z., 2022. Investigation of the renal protective effect of combined dietary polyphenols in streptozotocin-induced diabetic aged rats. Nutrients 14, 2867.

da Silva Reis, A.A., da Silva Santos, R., da Silva Cruz, A.H., da Silva, E.G., da Cruz, A.D., Pedrino, G.R., 2016. The effect of Nrf2 on diabetic complications. A MAster RegulAtor of OxidAtive Stress-The TrAnscription FActor Nrf2. IntechOpen.

Damasceno, D.C., Netto, A., Iessi, I., Gallego, F., Corvino, S., Dallaqua, B., Sinzato, Y., Bueno, A., Calderon, I.d.M.P., Rudge, M.V.C., 2014. Streptozotocin-induced diabetes models: Pathophysiological mechanisms and fetal outcomes. BioMed Res. Int. 2014.

Deng, Z., Hassan, S., Rafiq, M., Li, H., He, Y., Cai, Y., Kang, X., Liu, Z., Yan, T.,2020. Pharmacological activity of eriodictyol: The major natural polyphenolic flavanone. Evid. Based Complement. Alternat. Med. 2020.

Ding, Y., Li, H., Li, Y., Liu, D., Zhang, L., Wang, T., Liu, T., Ma, L., 2020. Protective effects of grape seed proanthocyanidins on the kidneys of diabetic rats through the Nrf2 signalling pathway. Evid.-Based Complement. Altern. Med. eCAM. 2020.

Dinkova-Kostova, A.T., Abramov, A.Y., 2015. The emerging role of Nrf2 in mitochondrial function. Free Radic. Biol. Med. 88, 179–188.

Dong, W., Jia, Y., Liu, X., Zhang, H., Li, T., Huang, W., Chen, X., Wang, F., Sun, W., Wu, H., 2017. Sodium butyrate activates NRF2 to ameliorate diabetic nephropathy possibly via inhibition of HDAC. J. Endocrinol. 232, 71–83.

Dufrane, D., van Steenberghe, M., Guiot, Y., Goebbels, R.-M., Saliez, A., Gianello, P., 2006. Streptozotocin-induced diabetes in large animals (pigs/primates): Role of GLUT2 transporter and β-cell plasticity. Transplantation 2006 (81), 36–45.

Eid, R.A., 2021. Acylated ghrelin protection inhibits apoptosis in the remote myocardium post-myocardial infarction by inhibiting calcineurin and activating ARC. Arch. Physiol. Biochem., 1–15.

Giwa, A.M., Ahmed, R., Omidian, Z., Majety, N., Karakus, K.E., Omer, S.M., Donner, T., Hamad, A.R.A., 2020. Current understandings of the pathogenesis of type 1 diabetes: genetics to environment. World J. Diabetes 11, 13.

Gomathi, D., Kalaiselvi, M., Ravikumar, G., Devaki, K., Uma, C., 2014. Evaluation of antioxidants in the kidney of streptozotocin induced diabetic rats. Indian J. Clin. Biochem. 29, 221–226.

Goodarzi, M.T., Navidi, A.A., Rezaei, M., Babahmadi-Rezaei, H., 2010. Oxidative damage to DNA and lipids: Correlation with protein glycation in patients with type 1 diabetes. J. Clin. Lab. Anal. 24, 72–76.

Graham, M.L., Janecek, J.L., Kittredge, J.A., Hering, B.J., Schuurman, H.-J., 2011. The streptozotocin-induced diabetic nude mouse model: Differences between animals from different sources. Comp. Med. 61, 356–360.

Gröne, H.-J., Walli, A.K., Gröne, E., Krämer, A., Clemens, M.R., Seidel, D., 1990. Receptor mediated uptake of apo B and apo E rich lipoproteins by human glomerular epithelial cells. Kidney Int. 37, 1449–1459.

Hernandez, L.F., Eguchi, N., Whaley, D., Alexander, M., Tantisattamo, E., Ichii, H., 2022. Anti-Oxidative therapy in diabetic nephropathy. Front. Biosci.-Sch. 14, 14.

Hirano, T., Satoh, N., Kodera, R., Hirashima, T., Suzuki, N., Aoki, E., Oshima, T., Hosoya, M., Fujita, M., Hayashi, T., 2022. Dyslipidemia in diabetic kidney disease classified by proteinuria and renal dysfunction: A cross-sectional study from a regional diabetes cohort. J. Diabetes Investig. 13, 657–667.

Hu, L.H., Liu, J.Y., Yin, J.B., 2021. Eriodictyol attenuates TNBS-induced ulcerative colitis through repressing TLR4/NF-kB signaling pathway in rats. Kaohsiung J. Med. Sci. 37, 812–818.

Huang, J., Tabbi-Anneni, I., Gunda, V.,Wang, L., 2010. Transcription factor Nrf2 regulates SHP and lipogenic gene expression in hepatic lipid metabolism. Am. J. Physiol.-Gastrointest. Liver Physiol. 299, G1211–G1221.

Huang, T.S., Wu, T., Wu, Y.D., Li, X.H., Tan, J., Shen, C.H., Xiong, S.J., Feng, Z.Q., Gao, S. F., Li, H., Cai, W.B., 2023. Long-term statins administration exacerbates diabetic nephropathy via ectopic fat deposition in diabetic mice. Nat. Commun. 14, 390.

Hung, P.-H., Hsu, Y.-C., Chen, T.-H., Lin, C.-L., 2021. Recent advances in diabetic kidney diseases: From kidney injury to kidney fibrosis. Int. J. Mol. Sci. 22, 11857.

Ishigaki, N., Yamamoto, T., Shimizu, Y., Kobayashi, K., Yatoh, S., Sone, H., Takahashi, A., Suzuki, H., Yamagata, K., Yamada, N., 2007. Involvement of glomerular SREBP-1c in diabetic nephropathy. Biochem. Biophys. Res. Commun. 364, 502–508.

Islam, M.T., 2020. Chemical profile and biological activities of Sonneratia apetala (Buch.-Ham.). Adv. Tradit. Med. 20, 123–132.

Jha, J.C., Banal, C., Chow, B.S., Cooper, M.E., Jandeleit-Dahm, K., 2016. Diabetes and kidney disease: Role of oxidative stress. Antioxid. Redox Signal. 25, 657–684.

Jiang, T., Huang, Z., Lin, Y., Zhang, Z., Fang, D., Zhang, D.D., 2010. The protective role of Nrf2 in streptozotocin-induced diabetic nephropathy. Diabetes 59, 850–860.

Jing, X., Ren, D., Wei, X., Shi, H., Zhang, X., Perez, R.G., Lou, H., Lou, H., 2013. Eriodictyol-7-O-glucoside activates Nrf2 and protects against cerebral ischemic injury. Toxicol. Appl. Pharmacol. 273, 672–679.

Jing, X., Shi, H., Zhu, X., Wei, X., Ren, M., Han, M., Ren, D., Lou, H., 2015. Eriodictyol Attenuates β-amyloid 25–35 peptide-induced oxidative cell death in primary cultured neurons by activation of Nrf2. Neurochem. Res. 40, 1463–1471.

Johnson, J., Maher, P., Hanneken, A., 2009. The flavonoid, eriodictyol, induces long-term protection in ARPE-19 cells through its effects on Nrf2 activation and phase 2 gene expression. Invest. Ophthalmol. Vis. Sci. 50, 2398–2406.

Kamanna, V.S., Pai, R., Roh, D.D., Kirschenbaum, M.A., 1996. Oxidative modification of low-density lipoprotein enhances the murine mesangial cell cytokines associated with monocyte migration, differentiation, and proliferation. Lab. Investig. A J. Tech. Methods Pathol. 74, 1067–1079.

Kandhare, A.D., Mukherjee, A., Bodhankar, S.L., 2017. Antioxidant for treatment of diabetic nephropathy: A systematic review and meta-analysis. Chem.-Biol. Interact. 278, 212–221.

Kashihara, N., Haruna, Y., Kondeti, V.K., Kanwar, Y.S., 2010. Oxidative stress in diabetic nephropathy. Curr. Med. Chem. 17, 4256–4269.

Kasiske, B.L., O'donnell, M.P., Cleary, M.P., Keane, W.F., 1988. Treatment of hyperlipidemia reduces glomerular injury in obese Zucker rats. Kidney Int. 33, 667–672.

Kavazis, A.N., 2009. Exercise preconditioning of the myocardium. Sport. Med. 39, 923–935.

Kawanami, D., Matoba, K., Utsunomiya, K., 2016. Dyslipidemia in diabetic nephropathy. Ren. Replace. Ther. 2, 1–9.

Khaki, A., Khaki, A.A., Hajhosseini, L., Golzar, F.S., Ainehchi, N., 2014. The antioxidant effects of ginger and cinnamon on spermatogenesis dys-function of diabetes rats. Afr. J. Tradit. Complement. Altern. Med. 11, 1–8.

Khan, N.U., Lin, J., Liu, X., Li, H., Lu, W., Zhong, Z., Zhang, H., Waqas, M., Shen, L., 2020. Insights into predicting diabetic nephropathy using urinary biomarkers. Biochim. Et Biophys. Acta (BBA)-Proteins Proteom. 1868, 140475.

Krämer, A., Nauck, M., Pavenstädt, H., Schwedler, S., Wieland, H., Schollmeyer, P., Wanner, C., 1993. Receptor-mediated uptake of IDL and LDL from nephrotic patients by glomerular epithelial cells. Kidney Int. 44, 1341–1351.

Kuwabara, T., Mori, K., Mukoyama, M., Kasahara, M., Yokoi, H., Saito, Y., Ogawa, Y., Imamaki, H., Kawanishi, T., Ishii, A., 2012. Exacerbation of diabetic nephropathy by hyperlipidaemia is mediated by Toll-like receptor 4 in mice. Diabetologia 55, 2256–2266.

Kwon, E.-Y., Choi, M.-S., 2019. Dietary eriodictyol alleviates adiposity, hepatic steatosis, insulin resistance, and inflammation in diet-induced obese mice. Int. J. Mol. Sci. 20, 1227.

Lee, S.E., Yang, H., Son, G.W., Park, H.R., Park, C.-S., Jin, Y.-H., Park, Y.S., 2015. Eriodictyol protects endothelial cells against oxidative stress-induced cell death through modulating ERK/Nrf2/ARE-dependent heme oxygenase-1 expression. Int. J. Mol. Sci. 16, 14526–14539.

Lenzen, S., 2008. The mechanisms of alloxan-and streptozotocin-induced diabetes. Diabetologia 51, 216–226.

Li, C.-Z., Jin, H.-H., Sun, H.-X., Zhang, Z.-Z., Zheng, J.-Z., Li, S.-H., Han, S.-H., 2016. Eriodictyol attenuates cisplatin-induced kidney injury by inhibiting oxidative stress and inflammation. Eur. J. Pharmacol. 772, 124–130.

Li, L., Li, W.-J., Zheng, X.-R., Liu, Q.-L., Du, Q., Lai, Y.-J., Liu, S.-Q., 2022. Eriodictyol ameliorates cognitive dysfunction in APP/PS1 mice by inhibiting ferroptosis via vitamin D receptor-mediated Nrf2 activation. Mol. Med. 28, 11.

Li, D., Mehta, J.L., 2000. Antisense to LOX-1 inhibits oxidized LDL–mediated upregulation of monocyte chemoattractant protein-1 and monocyte adhesion to human coronary artery endothelial cells. Circulation 101, 2889–2895.

Li, S., Zheng, L., Zhang, J., Liu, X., Wu, Z., 2021. Inhibition of ferroptosis by up-regulating Nrf2 delayed the progression of diabetic nephropathy. Free Radic. Biol. Med. 162, 435–449.

Lin, Y., Fang, J., Zhang, Z., Farag, M.A., Li, Z., Shao, P., 2022. Plant flavonoids bioavailability in vivo and mechanisms of benefits on chronic kidney disease: A comprehensive review. Phytochem. Rev., 1–25

Little, R.R., Rohlfing, C.L., Tennill, A.L., Hanson, S.E., Connolly, S., Higgins, T., Wiedmeyer, C.E., Weykamp, C.W., Krause, R., Roberts, W., 2013. Measurement of HbA1c in patients with chronic renal failure. Clin. Chim. Acta 418, 73–76.

Lou, H., Jing, X., Ren, D., Wei, X., Zhang, X., 2012. Eriodictyol protects against H2O2-induced neuron-like PC12 cell death through activation of Nrf2/ARE signaling pathway. Neurochem. Int. 61, 251–257.

Lv, P., Yu, J., Xu, X., Lu, T., Xu, F., 2019. Eriodictyol inhibits high glucose-induced oxidative stress and inflammation in retinal ganglial cells. J. Cell. Biochem. 120, 5644–5651.

Mahmoodnia, L., Aghadavod, E., Beigrezaei, S., Rafieian-Kopaei, M., 2017. An update on diabetic kidney disease, oxidative stress and antioxidant agents. J. Ren. Inj. Prev. 6, 153.

Mao, X., Jiang, Z., Shi, C., Lu, J., Rao, G., 2020. Eriodictyol attenuates spinal cord injury by activating Nrf2/HO-1 pathway and inhibiting NF-κB pathway. Trop. J. Pharm. Res. 19, 1611–1617.

Matoba, K., Takeda, Y., Nagai, Y., Kawanami, D., Utsunomiya, K., Nishimura, R., 2019. Unraveling the role of inflammation in the pathogenesis of diabetic kidney disease. Int. J. Mol. Sci. 20, 3393.

Matoba, K., Takeda, Y., Nagai, Y., Yokota, T., Utsunomiya, K., Nishimura, R., 2020. Targeting redox imbalance as an approach for diabetic kidney disease. Biomedicines. 8, 40.

Mestry, S.N., Dhodi, J.B., Kumbhar, S.B., Juvekar, A.R., 2017. Attenuation of diabetic nephropathy in streptozotocin-induced diabetic rats by Punica granatum Linn. leaves extract. J. Tradit. Complement. Med. 7, 273–280.

Miranda-Díaz, A.G., Pazarín-Villaseñor, L., Yanowsky-Escatell, F.G., Andrade-Sierra, J., 2016. Oxidative stress in diabetic nephropathy with early chronic kidney disease. J. Diabetes Res. 2016, 7047238.

Mitrofanova, A., Burke, G., Merscher, S., Fornoni, A., 2021. New insights into renal lipid dysmetabolism in diabetic kidney disease. World J. Diabetes 12, 524.

Mohan, T., Narasimhan, K.K.S., Ravi, D.B., Velusamy, P., Chandrasekar, N., Chakrapani, L.N., Srinivasan, A., Karthikeyan, P., Kannan, P., Tamilarasan, B., 2020. Role of Nrf2 dysfunction in the pathogenesis of diabetic nephropathy: Therapeutic prospect of epigallocatechin-3-gallate. Free Radic. Biol. Med. 160, 227–238.

Mohany, M., Alanazi, A.Z., Alqahtani, F., Belali, O.M., Ahmed, M.M., Al-Rejaie, S.S., 2020. LCZ696 mitigates diabetic-induced nephropathy through inhibiting oxidative stress, NF-κB mediated inflammation and glomerulosclerosis in rats. Peer. J. 8, e9196.

Mohany, M., Ahmed, M.M., Al-Rejaie, S.S., 2022a. The role of NF-κB and Bax/Bcl-2/Caspase-3 signaling pathways in the protective effects of sacubitril/Valsartan (Entresto) against HFD/STZ-Induced diabetic kidney disease. Biomedicines 10, 2863.

Mohany, M., Ahmed, M.M., Al-Rejaie, S.S., 2022b. Molecular mechanistic pathways targeted by natural antioxidants in the prevention and treatment of chronic kidney disease. Antioxidants. 11, 15.

Paik, S.-G., Fleischer, N., Shin, S.-I., 1980. Insulin-dependent diabetes mellitus induced by subdiabetogenic doses of streptozotocin: Obligatory role of cell-mediated autoimmune processes. PNAS 77, 6129–6133.

Pichler, R., Afkarian, M., Dieter, B.P., Tuttle, K.R., 2017. Immunity and inflammation in diabetic kidney disease: Translating mechanisms to biomarkers and treatment targets. Am. J. Physiol.-Ren. Physiol.312, F716–F731.

Quaschning, T., Königer, M., Krämer-Guth, A., Greiber, S., Pavenstädt, H., Nauck, M., Schollmeyer, P., Wanner, C., 1997. Receptor-mediated lipoprotein uptake by human glomerular cells: Comparison with skin fibroblasts and HepG2 cells. Nephrol. Dial. Transplant. Off. Publ. Eur. Dial. Transpl. Assoc.-Eur. Ren. Assoc. 12, 2528–2536.

Rico-Fontalvo, J., Aroca, G., Cabrales, J., Daza-Arnedo, R., Yánez-Rodríguez, T., Martínez-Ávila, M.C., Uparella-Gulfo, I., Raad-Sarabia, M., 2022. Molecular mechanisms of diabetic kidney disease. Int. J. Mol. Sci. 23, 8668.

Sampanis, C., 2008. Management of hyperglycemia in patients with diabetes mellitus and chronic renal failure. Hippokratia 12, 22.

Sanchez, M., Roussel, R., Hadjadj, S., Moutairou, A., Marre, M., Velho, G., Mohammedi, K., 2018. Plasma concentrations of 8-hydroxy-2'-deoxyguanosine and risk of kidney disease and death in individuals with type 1 diabetes. Diabetologia 61, 977–984.

Schelling, J.R., 2022. The contribution of lipotoxicity to diabetic kidney disease. Cells 11, 3236.

Scurt, F.G., Menne, J., Brandt, S., Bernhardt, A., Mertens, P.R., Haller, H., Chatzikyrkou, C., 2022. Monocyte chemoattractant protein-1 predicts the development of diabetic nephropathy. Diabetes Metab. Res. Rev. 38, e3497.

Selby, N.M., Taal, M.W., 2020. An updated overview of diabetic nephropathy: Diagnosis, prognosis, treatment goals and latest guidelines. Diabetes Obes. Metab. 22, 3–15.

Shawki, H.A., Elzehery, R., Shahin, M., Abo-Hashem, E.M., Youssef, M.M., 2021. Evaluation of some oxidative markers in diabetes and diabetic retinopathy. Diabetol. Int. 12, 108–117.

Shukla, R., Banerjee, S.,Tripathi, Y.B., 2018. Antioxidant and Antiapoptotic effect of aqueous extract of Pueraria tuberosa (Roxb. Ex Willd.) DC. On streptozotocin-induced diabetic nephropathy in rats. BMC Complement. Altern. Med. 18, 156.

Siddiqui, K., Joy, S.S., George, T.P., Mujammami, M., Alfadda, A.A., 2020. Potential role and excretion level of urinary transferrin, KIM-1, RBP, MCP-1 and NGAL markers in diabetic nephropathy. Diabetes Metab. Syndr. Obes. Targets Ther. 13, 5103.

Sugahara, M., Pak, W.L.W., Tanaka, T., Tang, S.C., Nangaku, M., 2021. Update on diagnosis, pathophysiology, and management of diabetic kidney disease. Nephrology 26, 491–500.

Sun, W., Liu, X., Zhang, H., Song, Y., Li, T., Liu, X., Liu, Y., Guo, L., Wang, F., Yang, T., 2017. Epigallocatechin gallate upregulates NRF2 to prevent diabetic nephropathy via disabling KEAP1. Free Radic. Biol. Med. 108, 840–857.

Tavafi, M., 2013. Diabetic nephropathy and antioxidants. J. Nephropathol. 2, 20.

Thimmulappa, R.K., Scollick, C., Traore, K., Yates, M., Trush, M.A., Liby, K.T., Sporn, M. B., Yamamoto, M., Kensler, T.W., Biswal, S., 2006. Nrf2-dependent protection from LPS induced inflammatory response and mortality by CDDO-Imidazolide. Biochem. Biophys. Res. Commun. 351, 883–889.

Thornalley, P.J., Rabbani, N., 2012. Dietary and synthetic activators of the antistress gene response in treatment of renal disease. J. Ren. Nutr. 22, 195–202.

Tuttle, K.R., Agarwal, R., Alpers, C.E., Bakris, G.L., Brosius, F.C., Kolkhof, P., Uribarri, J., 2022. Molecular mechanisms and therapeutic targets for diabetic kidney disease. Kidney Int. 102, 248–260.

Tuttle, K.R., Alicic, R.Z., 2021. Glycemic Variability and KIM-1–Induced Inflammation in the Diabetic Kidney. Diabetes. 70, 1617. (Jha et al., 2016; Tuttle and Alicic, 2021).

Ulasov, A.V., Rosenkranz, A.A., Georgiev, G.P., Sobolev, A.S., 2022. Nrf2/Keap1/ARE signaling: Towards specific regulation. Life Sci. 291, 120111.

Utsunomiya, K., Ohta, H., Kurata, H., Tajima, N., Isogai, Y., 1995. The effect of macrophage colony-stimulating factor (M-CSF) on the progression of lipid-induced nephrotoxicity in diabetic nephropathy. J. Diabetes Complicat. 9, 292–295.

Vodošek Hojs, N., Bevc, S., Ekart, R., Hojs, R., 2020. Oxidative stress markers in chronic kidney disease with emphasis on diabetic nephropathy. Antioxidants. 9, 925.

Wang, Y., Chen, Y., Chen, Y., Zhou, B., Shan, X., Yang, G., 2018. Eriodictyol inhibits IL-1β-induced inflammatory response in human osteoarthritis chondrocytes. Biomed. Pharmacother. 107, 1128–1134.

Wardyn, J.D., Ponsford, A.H., Sanderson, C.M., 2015. Dissecting molecular cross-talk between Nrf2 and NF-κB response pathways. Biochem. Soc. Trans. 43, 621–626.

Wei, P.Z., Szeto, C.C., 2019. Mitochondrial dysfunction in diabetic kidney disease. Clin. Chim. Acta 496, 108–116.

Wheeler, D., Fernando, R., Gillett, M., Zaruba, J., Persaud, J., Kingstone, D., Varghese, Z., Moorhead, J., 1991. Characterisation of the binding of low-density lipoproteins to cultured rat mesangial cells. Nephrol. Dial. Transplant. 6, 701–708.

Wu, J., Sun, X., Jiang, Z., Jiang, J., Xu, L., Tian, A., Sun, X., Meng, H., Li, Y., Huang, W., 2020. Protective role of NRF2 in macrovascular complications of diabetes. J. Cell Mol. Med. 24, 8903–8917.

Xing, L., Guo, H., Meng, S., Zhu, B., Fang, J., Huang, J., Chen, J., Wang, Y., Wang, L., Yao, X., 2021. Klotho ameliorates diabetic nephropathy by activating Nrf2 signaling pathway in podocytes. Biochem. Biophys. Res. Commun. 2021 (534), 450–456.

Yun, C., Lee, H.J., Lee, C.J., 2021. Eriodictyol inhibits the production and gene expression of MUC5AC mucin via the IκBα-NF-κB p65 signaling pathway in airway epithelial cells. Biomol. Ther. 29, 637.

Zhang, W.-Y., Lee, J.-J., Kim, Y., Kim, I.-S., Han, J.-H., Lee, S.-G., Ahn, M.-J., Jung, S.-H., Myung, C.-S., 2012. Effect of eriodictyol on glucose uptake and insulin resistance in vitro. J. Agric. Food Chem. 60, 7652–7658.

Zheng, H., Whitman, S.A., Wu, W., Wondrak, G.T., Wong, P.K., Fang, D., Zhang, D.D., 2011. Therapeutic potential of Nrf2 activators in streptozotocin-induced diabetic nephropathy. Diabetes 60, 3055–3066.

Zhu, G.F., Guo, H.J., Huang, Y., Wu, C.T., Zhang, X.F., 2015. Eriodictyol, a plant flavonoid, attenuates LPS-induced acute lung injury through its antioxidative and anti-inflammatory activity. Exp. Ther. Med. 10, 2259–2266.

Zoja, C., Xinaris, C., Macconi, D., 2020. Diabetic nephropathy: Novel molecular mechanisms and therapeutic targets. Front. Pharmacol. 11, 586892.